DINCON 2017
CONFERÊNCIA BRASILEIRA DE DINÂMICA, CONTROLE E APLICAÇÕES
30 de outubro a 01 de novembro de 2017 – São José do Rio Preto/SP

Analysis of the Impact of C_{22} on the Orbital Eccentricity of Spacecrafts Around Some Small Non-Spherical Celestial Bodies

Jean Paulo dos Santos Carvalho[1]
Centro de Ciência e Tecnologia em Energia e Sustentabilidade, UFRB, Feira de Santana, BA
Josué Cardoso dos Santos[2]
Department of Physics, School of Engineering, São Paulo State University (UNESP), Guaratinguetá, SP

Abstract. In this research, an analysis of the orbital eccentricity of an artificial satellite in motion around different small bodies of the solar system is performed. It is considered the disturbing effect due to some terms of the gravity potential related to the irregular shape of the central body. Emphasis is given on the impact caused by the C_{22} sectorial term. The J_2, J_3, J_4 zonal terms, due to the oblateness of the central body are considered in the dynamics. The study is performed under the assumption of single-averaged models for these perturbations and by mean their numerical propagation. We show that this C_{22} term generally acts as a protection mechanism against the growth of the eccentricity, which helps to control the increase of this orbital parameter when this perturbation is coupled with the other the perturbations considered.

Keywords. Astrodynamics, gravity potential, small bodies.

1 Introduction

In this work we consider the effects caused by the non-sphericity (J_2, J_3, J_4, and C_{22}) of the central body (here, assumed to be different small bodies of the solar system) on the orbital motion of an artificial satellite. Emphasis is given on the impact caused by the C_{22} sectorial term (equatorial ellipticity), which is explicitly time dependent, and affects significantly the evolution of the eccentricity of the orbit of a space vehicle. Each orbit around the central body is defined by mean of the parameters semimajor axis a, eccentricity e, inclination i, right ascension of the ascending node h, argument of the pericentre g and mean motion n. The lifetime of orbits for space missions around any celestial body is very dependent on the changes over the time in the eccentricity. Thus, there is an important aspect on orbital dynamics which is to investigate any natural

[1]jeanfeg@gmail.com
[2]josuesantosunesp@gmail.com

physical mechanism that can be able to protect the time increase of this parameter without the need of using the propulsion system of the spacecraft to save costs of operation during the mission. In order to investigate such kind of mechanism, we present an analytical theory using a single averaged model which is propagated through numerical simulations to investigate the impact of the C_{22} term on the orbital eccentricity of the artificial satellite. The idea is to analyze the effect of the zonal harmonics and the C_{22} sectoral term on the eccentricity of the artificial satellite for different small bodies of the solar system: one planet, six planetary moons and one dwarf planet. One of the first works dealing with the equatorial ellipticity of a celestial body was Sehnal (see Reference [10]), where the author considers the expression $h = h0 - wt$, here w is the rotation rate of the central body. This analytical expression for h is the same expression used in Reference [3] in the development of the equations of motion. In [9] the effect of the C_{22} term on orbit energy and angular momentum was analyzed. In this work, we consider tests for the following celestial bodies: the planet Mercury, the dwarf planet Haumea, the Moon of the Earth, the Galilean moons Europa, Ganymede and Callisto, and the moons of Saturn Rhea and Titan.

2 Nonsphericity of the Central Body

The disturbing potential due to the non-uniform distribution of mass of the central body up to the fourth order for the zonal terms and the C_{22} term is presented in References [2, 3, 12]. We get,

$$< R_{J2} >= -\tfrac{1}{4}\tfrac{J_2 R_e^2}{(1-e^2)^{3/2}} n^2(3s^2 - 2) \tag{1}$$

where R_e is the equatorial radius of the central body.

$$< R_{J3} >= -\tfrac{3}{8}\tfrac{J_3 R_e^3}{(1-e^2)^{5/2} a} n^2 se\sin(g)(5s^2 - 4) \tag{2}$$

$$\begin{aligned} < R_{J4} >= \tfrac{3}{128}\tfrac{J_4 R_e^4}{(1-e^2)^{7/2} a^2} n^2(140e^2 s^4(\cos(g))^2 - 120e^2 s^2(\cos(g))^2 - 175e^2 s^4 + \\ 180e^2 s^2 - 70s^4 - 24e^2 + 80s^2 - 16) \end{aligned} \tag{3}$$

$$< R_{C_{22}} >= -\tfrac{3}{2}\tfrac{C_{22} R_e^2}{(1-e^2)^{3/2}} n^2(c^2 - 1)\cos(2wt - 2h) \tag{4}$$

where $s = \sin i$ and $c = \cos i$. The parameter w is the mean motion of the central body [2, 4] or the rotation rate of the central body [2, 4]. For the sectorial perturbation see also Reference [12]. The development of these equations are presented in Reference [2].

Thus, the disturbing potential due to the effect of the non-spherical shape of the central body can be written as follows

$$R = \textstyle\sum_{n=2}^{4} < R_{Jn} > + < R_{C_{22}} > \tag{5}$$

Therefore, the motion of a artificial satellite is studied under a single-averaged analytical model considering the equations that represent the non-sphericity of the central bodoy (equations (1)-(4). The coefficients of the gravity field are given in Table 1 and Table 2. The references for the gravity coefficients are presented in the respective legends of each figure refereed to a specific celestial body. Note that in equation (4) the time appears explicitly on the right side. Replacing the potential given by equation (5) in the Lagrange planetary equations, we obtain a system of non-linear and non-autonomous differential equations. This system of differential equations is numerically integrated using a computer code developed for the Maple software.

Table 1: Values of the spherical harmonic coefficients.

Central Body	Mercury	Haumea	Moon	Europa
J_2	2.25045×10^{-5}	0.094995	2.032×10^{-4}	4.355×10^{-4}
J_3	4.76589×10^{-6}	—	8.475×10^{-6}	1.3784×10^{-4}
J_4	—	-0.040669	—	—
C_{22}	1.24538×10^{-5}	0.040669	2.447305×10^{-5}	1.3065×10^{-4}

Table 2: Values of the spherical harmonic coefficients.

Central Body	Ganymede	Callisto	Rhea	Titan
J_2	6.1436994×10^{-5}	1.545688×10^{-5}	9.31×10^{-4}	33.462×10^{-6}
J_3	-2.9029×10^{-6}	-7.574214×10^{-7}	2.5×10^{-5}	-0.074×10^{-6}
C_{22}	6.3943452×10^{-5}	1.6808453×10^{-5}	2.42×10^{-4}	10.022×10^{-6}

3 Results

The reason behind this different assumptions for the disturbing potential is to evaluate the influence due to C_{22} on increasing the value of the orbital eccentricity. Figures 1 to 10 show a comparison when the C_{22} term is taken into account in the dynamics and when this term is neglected.

Note that, in all cases, except the one shown in Figure 7, the C_{22} term acts as a "protection mechanism", helping on the control of the eccentricity growth. Only in the case of the Figure 7, the perturbation due to C_{22} term amplified the growth of the eccentricity. For the Saturn moon, Rhea, the effect of the C_{22} term only acts as a "protection mechanism" for values of the eccentricity higher than 0.0165.

The Figure 9 shows the behavior of the eccentricity versus the argument of the pericentre for the Ganymede natural satellite. Note that some orbits librates around the equilibrium point, especially $e = 0.018$ which shows less variation of the orbital elements, others are oscillating. The characteristic of the orbit with smaller amplitude of variation is important for scientific missions, since it can contribute to reduce the consumption of fuels with orbits corrections.

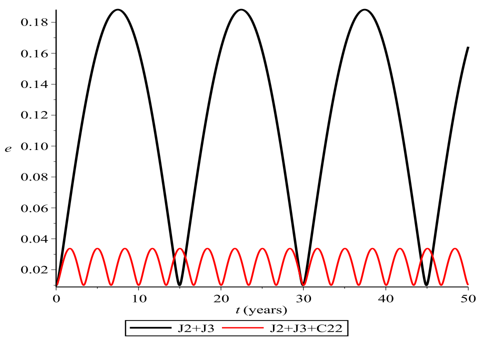

Figure 1: $e \times t$ (Mercury). Initial conditions: $a = 2740$ km, $e = 0.01$, $i = 90°$, $g = 270°$, $h = 90°$, $R_e = 2440$ km, $w = 0.1212 \times 10^{-5}$ rad/s. Perturbations: $J_2 + J_3 + C_{22}$. Reference [7].

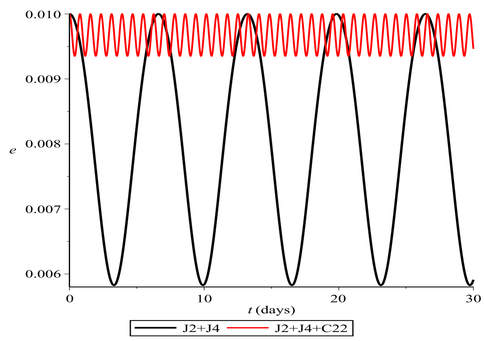

Figure 2: $e \times t$ (Haumea). Initial conditions: $a = 1450$ km, $e = 0.01$, $i = 90°$, $g = 270°$, $h = 90°$, $R_e = 1250$ km, $w = 6.9749 \times 10^{-10}$ rad/s. Perturbations: $J_2 + J_4 + C_{22}$. Reference [8].

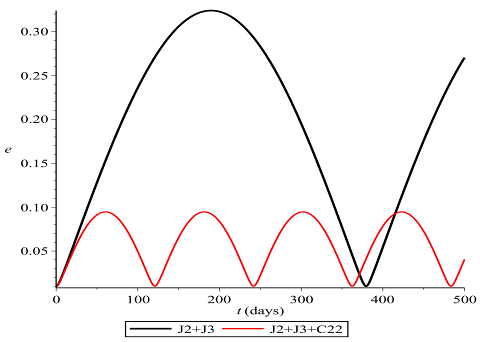

Figure 3: $e \times t$ (Europa). Initial conditions: $a = 1710.8$ km, $e = 0.01$, $i = 90°$, $g = 270°$, $h = 90°$, $R_e = 1560.8$ km, $w = 2.0477 \times 10^{-5}$ rad/s. Perturbations: $J_2 + J_3 + C_{22}$. Reference [3].

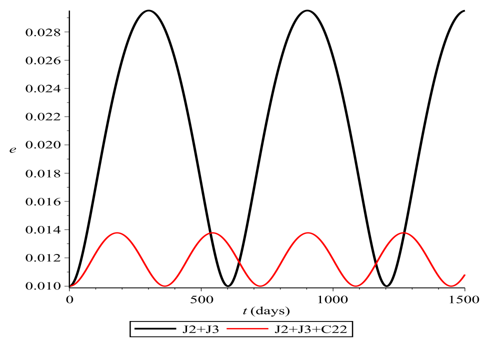

Figure 4: $e \times t$ (Moon). Initial conditions: $a = 1838$ km, $e = 0.01$, $i = 90°$, $g = 270°$, $h = 90°$, $R_e = 1738$ km, $w = 0.2714 \times 10^{-5}$ rad/s. Perturbations: $J_2 + J_3 + C_{22}$. Reference [6].

4 Conclusions

In this work we analyze the effect of the non-sphericity of the central body on the orbital motion of artificial satellites. Emphasis is given to the gravity term known as C_{22}, which is the term related to the equator's elliptical shape of the central body. We consider numerical simulations for the following celestial bodies: planet Mercury, the dwarf planet Haumea, the Moon of the Earth, the Galilean moons Europa, Ganymede and Callisto and the moons of Saturn Titan and Rhea. We present a comparison when the effect

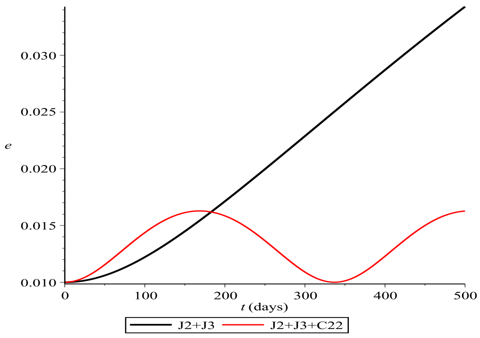

Figure 5: $e \times t$ (Ganymede). Initial conditions: $a = 2731.2$ km, $e = 0.01$, $i = 90°$, $g = 270°$, $h = 90°$, $R_e = 2631.2$ km, $w = 0.1016 \times 10^{-4}$ rad/s. Perturbations: $J_2 + J_3 + C_{22}$. Reference [1].

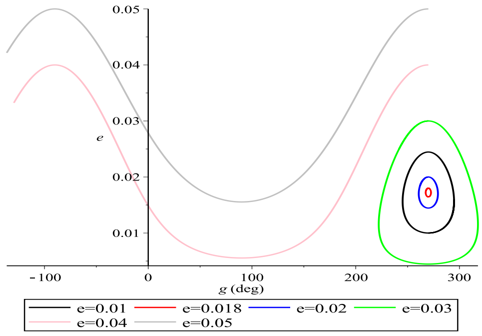

Figure 6: $e \times g$ (Ganymede). Initial conditions: $a = 2731.2$ km, $i = 90°$, $g = 270°$, $h = 90°$, $R_e = 2631.2$ km, $w = 0.1016 \times 10^{-4}$ rad/s. Perturbations: $J_2 + J_3 + C_{22}$. Reference [1].

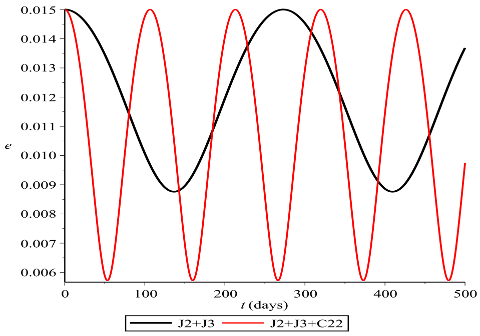

Figure 7: $e \times t$ (Rhea). Initial conditions: $a = 864.3$ km, $e = 0.015$ $i = 90°$, $g = 270°$, $h = 90°$, $R_e = 764.3$ km, $w = 1.6098 \times 10^{-5}$ rad/s. Perturbations: $J_2 + J_3 + C_{22}$. Reference [11].

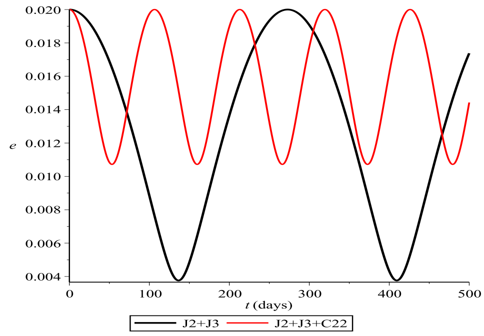

Figure 8: $e \times t$ (Rhea). Initial conditions: $a = 864.3$ km, $e = 0.02$, $i = 90°$, $g = 270°$, $h = 90°$, $R_e = 764.3$ km, $w = 1.6098 \times 10^{-5}$ rad/s. Perturbations: $J_2 + J_3 + C_{22}$. Reference [11].

due to the C_{22} term is neglected with the case when this effect is taken into account in the dynamics. The orbital element analyzed is the eccentricity of the spacecraft, which impacts important issues as the survival time of orbits for space missions around a central body with irregular shape, precisely the case for the bodies considered in the present investigation. The eccentricity growth rate is reduced when we consider J_2, J_3 and J_4 coupled with the C_{22} term in the disturbing potential. Only in the case of the moon of Saturn Rhea, where the rate of growth of the eccentricity is amplified from the initial value of 0.015. However, we note that by choosing the initial eccentricity as 0.0165, the effect

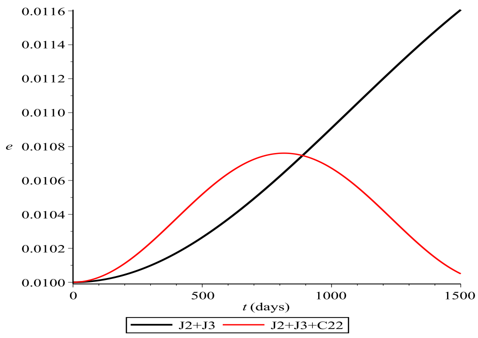

Figure 9: $e \times t$ (Titan). Initial conditions: $a = 2675$ km, $e = 0.01$, $i = 90°$, $g = 270°$, $h = 90°$, $R_e = 2575$ km, $w = 4.5607 \times 10^{-6}$ rad/s. Perturbations: $J_2 + J_3 + C_{22}$. Reference [5].

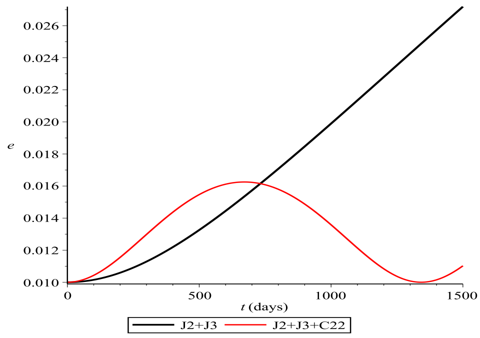

Figure 10: $e \times t$ (Callisto). Initial conditions: $a = 2510.3$ km, $e = 0.01$, $i = 90°$, $g = 270°$, $h = 90°$, $R_e = 2410.3$ km, $w = 4.3575 \times 10^{-6}$ rad/s. Perturbations: $J_2 + J_3 + C_{22}$. Reference [1].

due to C_{22} again contributed to reduce the increase of the eccentricity, as it happened with the simulations performed considering the other bodies.

In general, we show that the term due to equatorial ellipticity (C_{22}) acts as a protection mechanism in the control of the orbital eccentricity of the artificial satellite. This fact indicates that the coupling of the perturbations considered in the problem helps to control the increase in eccentricity and thereby, this coupling reduces the cost with necessary orbital corrections. We also note that, in addition to the case of the moon Rhea, there are some other cases where the C_{22} term can amplify the growth of the eccentricity, which is dependent on the initial value considered for the eccentricity. In the continuation of this work we will analyze in more detail the contribution of the C_{22} term to different initial values of the eccentricity and try to find a relation between the two parameters.

Acknowledgements

Sponsored by CNPq - Brazil. The authors are grateful to CNPq (National Council for Scientific and Technological Development) and FAPESP (São Paulo Research Foundation) - Brazil for contracts 306953/2014-5, 420674/2016-0 (CNPq) and 2013/26652-4 (FAPESP).

References

[1] J. Aiello, Numerical Investigation of Mapping Orbits about Jupiter's Icy Moons, Paper AAS 2005-377, 2005.

[2] J. P. S. Carvalho, E. Tresaco, R. Vilhena de Moraes e A. F. B. A. Prado, Perturbações orbitais sobre uma vela solar, Proceeding Series of the Brazilian Society of Computational and Applied Mathematics, vol. 5, (2017), DOI: 10.5540/03.2017.005.01.0191.

[3] J. P. S. Carvalho, R. Vilhena de Moraes and A. F. B. A. Prado, Dynamics of artificial satellites around Europa, Mathematical Problems in Engineering, Vol. 2013, Article ID 182079, 7 pages, (2013), DOI: 0.1155/2013/182079.

[4] G. E. O. Giacaglia, J. Murphy and T. Felsentreger, A semi-analytic theory for the motion of a lunar satellite, Celest. Mech., vol. 1, 3–66, (1970).

[5] L. Iess, N. J. Rappaport, R. A. Jacobson et al., Gravity Field, Shape, and Moment of Inertia of Titan, Science, vol. 327, 1367–1369, (2010).

[6] A. S. Konopliv, S. W. Asmar, E. Carranza, W. L. Sjogren and D. N. Yuan. Recent gravity models as a result of the lunar prospector mission, Icarus, vol. 150, 1–18, (2001).

[7] E. Mazarico, A. Genova, S. Goossens, et al., The gravity field, orientation, and ephemeris of Mercury from MESSENGER observations after three years in orbit, Jounal of Geophys. Res. Planets, vol. 119, 2417–2436, (2014).

[8] D. M. Sanchez, Estudo de captura gravitacional e custos de manutenção orbital em dinâmicas não keplerianas, Tese de Doutorado, INPE, (2015).

[9] D. J. Scheeres, The effect of C_{22} on orbit energy and angular momentum, Celest. Mech. Dyn. Astron., vol. 73, 339–348, (1999).

[10] L. Sehnal, The influence of the equatorial ellipticity of the Earth gravitational field on the motion of a close satellite, Bulletin of the Astronomical Institute of the Czechoslovak Academy of Sciences, vol. 11, 90–93, (1959).

[11] P. Tortora, M. Zannoni, D. Hemingway, et al., Rhea gravity gravity field and interior modeling from Cassini data analysis, Icarus, vol. 264, 264-273, (2016).

[12] E. Tresaco, J. P. S. Carvalho, A. Elipe, A. F. B. A. Prado and R. Vilhena de Moraes, Averaged model to study long-term dynamics of a probe about Mercury, (2017) (To appear).